Method for cooling nanostructures to microkelvin temperatures

A. C. Clark,[a] K. K. Schwarzwälder,[a] T. Bandi, D. Maradan, and D. M. Zumbühl[b]
Department of Physics, University of Basel, Klingelbergstrasse 82, Basel CH-4056, Switzerland

(Received 1 July 2010; accepted 25 August 2010; published online 25 October 2010)

We propose a new scheme aimed at cooling nanostructures to microkelvin temperature based on the well established technique of adiabatic nuclear demagnetization: we attach each device measurement lead to an individual nuclear refrigerator, allowing efficient thermal contact to a microkelvin bath. On a prototype consisting of a parallel network of nuclear refrigerators, temperatures of ~1 mK simultaneously on ten measurement leads have been reached upon demagnetization, thus completing the first steps toward ultracold nanostructures. © *2010 American Institute of Physics.* [doi:10.1063/1.3489892]

I. INTRODUCTION

The ability to reach low millikelvin or even microkelvin temperatures in nanoscale samples would open up the possibility to discover new physics in a variety of systems. For example, an intriguing nuclear spin ferromagnetic phase transition in a GaAs interacting 2D electron gas (2DEG) has been predicted[1,2] to occur around ~1 mK at $B=0$, constituting a novel type of correlated state. Nuclear spin fluctuations would be fully suppressed in this ferromagnetic phase, eliminating the main source of decoherence for GaAs spin qubits.[3] Further, full thermodynamic nuclear polarization is possible[4] at temperatures $T \lesssim 1$ mK in an external magnetic field of $B \sim 10$ T. Other systems benefiting from ultralow temperatures include fractional quantum hall states with small gaps,[5,6] in particular the $\nu=5/2$ state,[7] which is currently considered for topological quantum computation.[8,9]

The majority of quantum transport experiments to date, such as those in GaAs 2DEGs or any other nanoelectronic devices on insulating substrates, have been carried out at electron temperatures T_e significantly greater than that of the host ^{3}He–^{4}He dilution refrigerator (DR). Since only metals provide significant thermal conduction at temperatures well below 1 K,[10,11] nanostructures are thermally connected to and cooled by the DR primarily through their electrical leads. Since these leads need to be electrically isolated, some insulator will still inhibit efficient cooling. The main challenges for cooling such samples below 1 mK include overcoming poor thermal coupling between electrons in the leads and the refrigerator,[12,13] providing sufficient attenuation of high frequency radiation, and reducing low frequency interference such as ground loops. To our knowledge, the minimum temperature reported is 4 mK, with sintered silver heat exchangers attached to sample wires in a ^{3}He cell.[5,6] Similarly, Pomeranchuck cooling[11] with sinters on each sample wire could reach temperatures ~1 mK.

Here we present a new method intended to cool nanostructures into the microkelvin regime. We propose to adapt the very well established technique of nuclear adiabatic demagnetization to the specific needs of nanoscale samples: every sample wire passes through its own, separate nuclear refrigerator (NR) (see Fig. 1), ensuring excellent thermal contact even at microkelvin temperatures between the sample and the NR while keeping all wires electrically isolated from one another, as required for measurements. With this method, nanostructures can in principle be cooled to less than 100 μK, which would be a reduction in temperature by more than two orders of magnitude compared with common $T_e \gtrsim 10$ mK. Further, we have designed, built, and tested a prototype refrigerator that is based on this proposal. We present evidence for achieving ~1 mK in ten NRs simultaneously, thus completing the first steps toward microkelvin nanostructures.

Nuclear adiabatic demagnetization is the most widely used technique available today for ultralow temperature experiments in condensed matter.[10,11,14] The lowest temperatures reported are ~1 μK for electrons in platinum[15] and ~300 pK for nuclear spins in rhodium,[16,17] among the low-

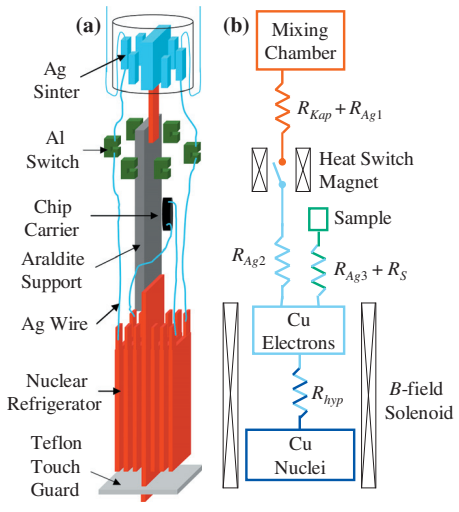

FIG. 1. (Color) (a) Schematic of parallel nuclear refrigerator network (not to scale). Only six NRs are shown for simplicity. The Cu pieces are $10\times2\times0.2$ cm^3 and positioned approximately 35 cm from the bottom of the MC. (b) Cooling scheme, with different colors denoting potentially different temperatures under steady state conditions.

[a]These authors contributed equally to this work.
[b]Electronic mail: dominik.zumbuhl@unibas.ch.

est temperatures achieved in any laboratory. It is a single shot method consisting of three steps. First, a suitable metal with nonzero nuclear spin (the NR) is precooled with a DR in a large magnetic field B_i to a temperature $T_i \sim 10$ mK, generating as large a thermodynamic nuclear spin polarization as possible. Second, thermal contact between the DR and NR is cut off by a superconducting heat switch and the B-field is adiabatically reduced by a large factor, e.g., $x = B_i/B_f \sim 100$. Ideally (perfect adiabaticity), the nuclei are cooled by the same factor such that $T_f = T_i/x$. Finally, experiments are performed at microkelvin temperatures for a finite time, typically days or even weeks. The heat leaking into the system plays an important role since it increases T_e in the NRs above the nuclear spin temperature and is absorbed by the nuclei until the polarization is lost and the NRs heat up to or above DR temperatures.

We propose to cool nanostructures to microkelvin temperatures using a parallel network of NRs. Each NR constitutes part of the electrical connection from room temperature down to the sample. Semiconductors and insulators, commonly used in nanosamples, are not practical as NRs since it is difficult to sufficiently precool their nuclei. Still, one might consider as NRs devices with large conducting regions containing nuclear spins, such as GaAs 2DEGs with a highly doped, metallic back gate (or similar). However, their nuclear heat capacity would be drained all too quickly given realistic heat leaks and 2DEG piece sizes. Therefore, our strategy is to incorporate the most widely used material for NRs: Cu, an excellent conductor with nuclear spin 3/2. In this system the nuclear hyperfine interaction couples the nuclei at temperature T_f to the electrons at temperature T_e with a characteristic nuclear spin relaxation time T_1 that obeys the Korringa law,[10,11] $T_e T_1 = \kappa \approx 1$ K s. The effective thermal equilibration time is reduced from T_1 by the very large ratio of nuclear and electronic heat capacities,[18] resulting in strong, fast coupling even at $T_e < 100$ μK. However, conducting sample sections may be thermally isolated from other degrees of freedom at low enough temperatures.

II. NUCLEAR REFRIGERATOR NETWORK

We now turn to the discussion of the prototype NR network (see Fig. 1). Each NR consists of a Cu plate situated in the center of a demagnetizing field, connected with high conductivity wires on one side to a home built chip carrier made from 2850 FT Stycast epoxy,[19] and on the other side through a heat switch[20] to the mixing chamber (MC) of a DR. Twelve parallel NRs are tied to a sacrificial NR with dental floss, using small Teflon spacers ensuring electrical (and thermal) isolation, giving a total of 13 NRs. The sacrificial Cu piece is glued into an araldite[21] beam extending from the MC. A Teflon touch guard is positioned at the bottom of the sacrificial piece to prevent the NRs from contacting the 50 mK shield of the DR. The shield serves two purposes: to reduce black-body radiation from higher temperature stages of the cryostat and to protect from stray radio-frequency (rf) noise sources.

To ensure proper operation of the NRs, we note some important details. Each measurement wire begins with 1.6 m of lossy Thermocoax[22] extending from room temperature down to the MC cold finger. It then passes through a silver epoxy microwave filter[23] and is transferred to a bare Ag wire that is fed directly into the plastic MC. These two filtering steps are important for reducing the rf noise dropping across the device. For efficient thermalization of the Cu during precooling the thermal resistance between the NR and MC must be minimized. We therefore use annealed, high purity Ag wire with 1.27 mm diameter, and residual resistivity ratio ≥ 1500, which are spot welded to the Cu pieces and, in the MC, sintered to Ag nanoparticles (yielding surface areas of ~ 3 m^2 per wire used to overcome the Kapitza resistance R_{Kap}). The heat switches are "C"-shaped pieces of annealed, high purity Al fused to the Ag wires on both ends. The small critical field of 10 mT allows easy switching with a home built magnet. The ratio of thermal conductivities in the closed state (Al normal) to the open state (Al superconducting) exceeds 10^4 below 20 mK. Al pieces are placed carefully to minimize differences in the stray B-field from the solenoid, adding additional complexity for a network of NRs.

The entire stage is removable at a plastic cone seal at the MC, allowing samples to be directly wire bonded to polished Ag wires. Probably the weakest thermal/electrical link between the device and the NR occurs at the Schottky barriers of the metal-semiconductor contacts, integrated on chip. In steady state, parasitic heat leaking into the device will equal the heat leaving it through its thermal links to the NRs, setting the lowest achievable temperature. Metallic nanostructures will benefit from comparatively higher conductivity metal-metal contacts.

III. THERMOMETRY AND HEAT LEAK

Characterization of the NRs has been carried out by monitoring T_e of the various Cu plates. Five RuO_2 chip resistors, labeled A–E, were mounted on the chip carrier [see Fig. 2(a) inset] and electrically connected[24] to 10 of the 13 NRs, with each chip using a pair of NRs as its leads. The resistance reading in these cases reflects an "average" temperature of each pair. Two more chips, F and S, were directly mounted onto individual NRs (S on the sacrificial Cu plate), with the second contact of each electrically connected to, but thermally isolated from, the outside world by a bare NbTi superconducting wire. The final plate was left unmonitored, serving as electrical ground (G) for chip capacitors across A and B. It is well known that RuO_2 thermometers can suffer from rather long time constants[25] and saturate below 10 mK. However, in the demagnetized state, we can extrapolate the NR temperatures below 10 mK based on warm up curves, as will be described below.

We first calibrate the RuO_2 thermometers between 12 and 120 mK. Figure 2(a) shows the resistance of the seven RuO_2 chips at $B=0$ as a function of mixing chamber temperature T_{MC} with Al switches closed. T_{MC} was measured by a cerium magnesium nitrate (CMN) thermometer bolted to the MC cold finger. Before measuring each data point, an appropriate amount of time for thermalization was allowed. There is no apparent saturation down to $T_{\mathrm{MC}} = 12$ mK for

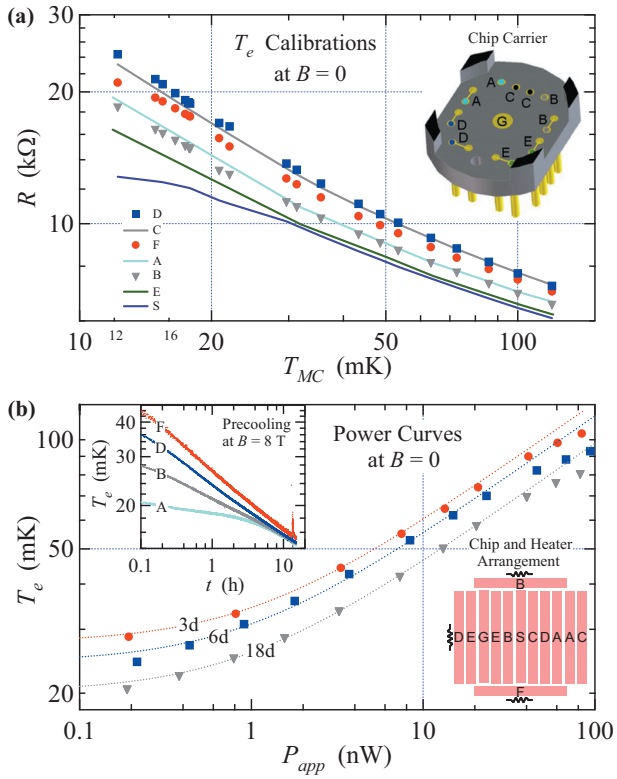

FIG. 2. (Color) (a) Resistance of RuO_2 chips as a function of T_{MC}. Inset: chip carrier (to scale). It is 2 cm across from one flat to the other. The bond pads are polished Ag wires, 1.27 mm in diameter. (b) Power curves with Al switches open measured 3, 6, and 18 days after cooling down, shown for chips F (circles), D (squares), and B (triangles), respectively. Dashed lines are theory (see text). Left inset: T_e vs time during precooling (B=8 T). Right inset: arrangement of Cu plates in the NR stack.

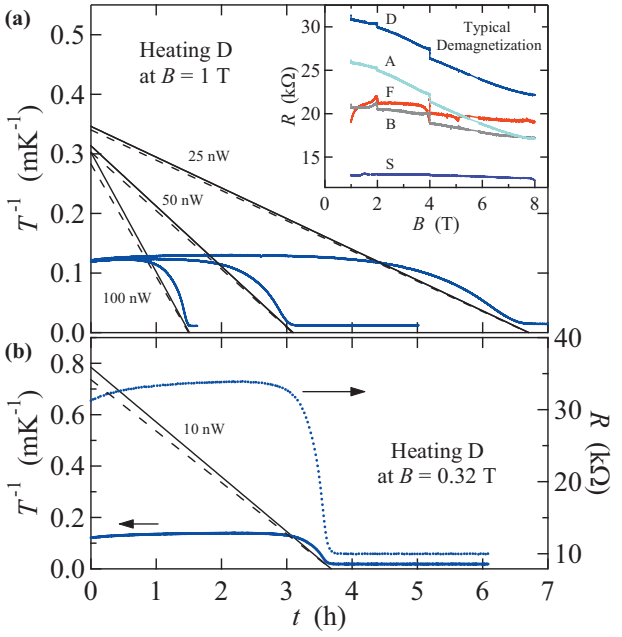

FIG. 3. (Color) (a) Systematic heating tests for chip D after demagnetization. Measured T_e^{-1} (blue curves) and theory for T_f^{-1} (solid lines) and T_e^{-1} (dashed lines) vs t for the applied powers indicated. Inset: cooling of chips during demagnetization. R of thermometer D is plotted against the right axis for comparison in (b).

thermometers A–F, which all exhibit qualitatively the same temperature dependence. Moreover, on two separate cooldowns a second CMN was mounted directly onto one of the NRs (first A, then F), verifying that T_e measured by the RuO_2 chips is indeed equal to T_{MC}.[26] We therefore use the data in Fig. 2(a) as electron temperature calibrations for NRs A–F. The sacrificial plate thermometer S displays some saturation for $T_{MC} \leq 30$ mK, presumably due to a heat leak. Upon ramping the magnet to B=8 T, the massive nuclear heat of magnetization significantly elevates the NR temperatures (varying somewhat for individual plates depending on stray B-field conditions at the corresponding heat switches), but they cool within 15 h to $T_i = T_e \leq 15$ mK [see Fig. 2(b) left inset].

Next, we measure the parasitic heat leak to the NRs. Figure 2(b) shows the NR temperature T_e as a function of applied power at B=0 and with the Al switches open. The heat flowing into the Cu is ultimately drained away by the MC, with the superconducting Al piece as the primary impedance. Its thermal conductance is dominated at low temperature by phonon-dislocation scattering processes, obeying the relation[11,27] $P_{app} = nA(T_e^3 - T_{MC}^3) - P_0$, where P_{app} is the applied power, n=0.57 mol of Cu, A is a prefactor, and P_0 is the intrinsic heat leak to the NR. For $T_e > 70$ mK, parallel channels of heat flow become accessible.[28] Fits (dashed curves) are in very good agreement with the data and allow us to extract P_0, which improved over time as indicated by the decrease in T_e (true for *all* chips A–F) as $P_{app} \to 0$ in the power curves obtained 3, 6, and 18 days after cooling down (top to bottom curves). We conclude that the typical intrinsic heat leak to the NR stage at B=0 is $P_0/n \lesssim 1$ nW mol^{-1}, sufficiently low but clearly above the state of the art value[18] of <5 pW mol^{-1}. We note that the average heat leak measured at B=2 T is ~ 7 nW mol^{-1}, which is most likely from eddy currents in the Cu pieces generated by small vibrations in the nonuniform B-field.

IV. PERFORMANCE

Given a heat leak sufficiently low for nuclear cooling, we now evaluate the demagnetization process itself, starting from T_i=15 mK and B_i=8 T. The inset of Fig. 3 shows the resistance of several chips during a series of ramps from 8 T $\to$ 1 T with open heat switches. The B-field is decreased linearly in time using three sequential ramps at 1 T h^{-1} from 8 T $\to$ 4 T, and at 0.5 T h^{-1} from 4 T $\to$ 2 T and 2 T $\to B_f$=1 T. R values increase upon demagnetization, clearly indicating cooling. They continue to increase (at fixed values of 4 and 2 T) between each B-field ramp and in fact do so more quickly, reflecting both a thermal lag between the chips and Cu plates as well as a sensitivity to ramp rate. If enough time is allowed after reaching 1 T, R increases further by 5 to 10 kΩ for chips A–E (not shown). Chip F warms up near the end of the demagnetization, while S is nearly constant. The apparently higher heat load on F seems to be associated with vibrations.[29] However, its performance improves for lower precooling temperatures. For S, the lack of cooling *and* warming suggest that thermal contact to the environment remains significant.

We extract T_f and $T_e (\gtrsim T_f)$ of the NRs reached after demagnetizing to B_f by recording the time t necessary for a

Cu plate to "completely" ($T_e^{-1} \to 0$) warm up under an applied power, using $t = n\Lambda B_f^2/(P_{\text{app}} T_f)$ and $T_e = T_f(1 + \kappa P_{\text{app}}/n\Lambda B_f^2)$, where Λ is the nuclear Curie constant for Cu.[11,18] In Fig. 3(a) we plot time traces of T_e^{-1} for chip D (not calibrated above 0.08 mK^{-1}) for $P_{\text{app}} = 25$, 50, and 100 nW. The other thermometers give consistent results, except for F, which appears to heat up during demagnetization. Due to poor internal thermalization T_e^{-1} increases for the first several hours despite the influx of heat, only showing significant signs of warming once the Cu is hotter than ~10 mK. Since the temperature gradient between the chip and NR will vanish at $T_f^{-1} = T_e^{-1} = 0$, we fix this point of the theoretical T^{-1} curves (solid and dashed lines) and extrapolate back to $t = 0$. As expected, larger P_{app} results in faster warm up times. With this, we obtain $T_f(0) = 3.0 \pm 0.3$ mK for all three P_{app}, demonstrating the reliability of achieving a particular minimum temperature for a set of demagnetization parameters. The uncertainty in $T_f(0)$ is dominated by the inhomogeneity of B_f. We note that in the temperature range explored here, $T_e(0) \approx T_f(0)$ before the power is turned on since $P_0 \ll P_{\text{app}}$.

The final test from the present work [see Fig. 3(b)] is a demagnetization from 8 T → 0.32 T starting at 13.3 mK and cooling to 1.2 ± 0.1 mK (extracted using the method described above), demonstrating a reduction in temperature upon demagnetization by a factor of 10. The other chips perform similar to D, thus substantiating the overall cooling scheme proposed here for reaching submillikelvin temperatures on multiple measurement leads.

Ideally, T_i of the Cu nuclei will be reduced by the same factor x as the B-field. To characterize the demagnetization process we introduce the efficiency $\xi_{B_f} = T_i/T_f \div B_i/B_f$ and find $\xi_{4T} = 88 \pm 3\%$, $\xi_{2T} = 80 \pm 3\%$, $\xi_{1T} = 63 \pm 3\%$, and $\xi_{0.3T} = 42 \pm 2\%$. $\xi < 100\%$ signifies nonadiabadicity, which becomes worse at lower magnetic field due to the smaller heat capacity of the nuclei (proportional to B_f^2). The dominant loss mechanism has been identified as a heat leak due to sweeping the B-field. We determined the magnitude to be ~20 nW (>35 nW mol^{-1}) at 1 T h^{-1} and ~10 nW (>18 nW mol^{-1}) at 0.5 T h^{-1}, which are 20 and 40 times greater than expected from a simple calculation of eddy currents.[11] The cause of the heat leak is presently unclear and under investigation.

V. CONCLUSIONS

In conclusion, we have laid out a method that enables the direct and simultaneous cooling of the electrical leads to a nanoscale device. Its strength is that it short circuits the two main bottlenecks of cooling electrons: thermal boundary resistance and electron-phonon coupling. We have addressed the technical challenges of constructing a parallel NR network, yielding a prototype that achieves a base temperature of ~1 mK. Future efforts will reduce the intrinsic heat leak and address the presently low efficiency (securing temperatures well within the microkelvin regime), further demonstrate ultralow temperatures directly in nanoscale devices, and add an independently controllable magnetic field for the sample.

ACKNOWLEDGMENTS

We thank G. R. Pickett, R. P. Haley, M. Paalanen, R. Blaauwgeers, G. Frossati, and A. de Waard for their advice. This work was supported by the Swiss Nanoscience Institute, Swiss NSF, ERC Starting Grant, and EU-FP7 MICROKELVIN network.

[1] P. Simon and D. Loss, Phys. Rev. Lett. **98**, 156401 (2007).
[2] P. Simon, B. Braunecker, and D. Loss, Phys. Rev. B **77**, 045108 (2008).
[3] R. Hanson, L. P. Kouwenhoven, J. R. Petta, S. Tarucha, and L. M. K. Vandersypen, Rev. Mod. Phys. **79**, 1217 (2007).
[4] S. Chesi and D. Loss, Phys. Rev. Lett. **101**, 146803 (2008).
[5] W. Pan, J. S. Xia, V. Shvarts, D. E. Adams, H. L. Störmer, D. C. Tsui, L. N. Pfeiffer, K. W. Baldwin, and K. W. West, Phys. Rev. Lett. **83**, 3530 (1999).
[6] J. S. Xia, D. E. Adams, V. Shvarts, W. Pan, H. L. Störmer, and D. C. Tsui, Physica B **280**, 491 (2000).
[7] R. Willett, J. P. Eisenstein, H. L. Störmer, and D. C. Tsui, Phys. Rev. Lett. **59**, 1776 (1987).
[8] A. Yu. Kitaev, Ann. Phys. **303**, 2 (2003).
[9] C. Nayak, S. H. Simon, A. Stern, M. Freedman, and S. Das Sarma, Rev. Mod. Phys. **80**, 1083 (2008).
[10] O. V. Lounasmaa, *Experimental Principles and Methods Below 1K* (Academic, London, 1974).
[11] F. Pobell, *Matter and Methods at Low Temperatures* (Springer, Berlin, 2007).
[12] Y. C. Chung, M. Heiblum, and V. Umansky, Phys. Rev. Lett. **91**, 216804 (2003).
[13] R. M. Potok, I. G. Rau, H. Shtrikman, Y. Oreg, and D. Goldhaber-Gordon, Nature (London) **446**, 167 (2007).
[14] G. R. Pickett, Rep. Prog. Phys. **51**, 1295 (1988).
[15] W. Wendler, T. Herrmannsdörfer, S. Rehmann, and F. Pobell, Europhys. Lett. **38**, 619 (1997).
[16] T. A. Knuuttila, J. T. Tuoriniemi, K. Lefmann, K. I. Juntunen, F. B. Rasmussen, and K. K. Nummila, J. Low Temp. Phys. **123**, 65 (2001).
[17] P. J. Hakonen, R. T. Vuorinen, and J. E. Martikainen, Phys. Rev. Lett. **70**, 2818 (1993).
[18] G. R. Pickett, Physica B **280**, 467 (2000).
[19] R. P. Haley (personal communication), 2008.
[20] N. S. Lawson, Cryogenics **22**, 667 (1982).
[21] Supplied by Huntsman Advanced Materials GmbH.
[22] A. B. Zorin, Rev. Sci. Instrum. **66**, 4296 (1995).
[23] C. Scheller, S. Heizmann, and D. M. Zumbühl (unpublished).
[24] The (superconducting) tin on the pads of the RuO_2 chips was removed. Contact was made using Ag epoxy.
[25] The total thermal equilibration times for the chips are 20 min at 30 mK, 120 min at 15 mK, and >4 h at 5 mK.
[26] The NR was able to cool the CMN to ≤3 mK. However, a heat leak of >20 nW was detected from the thermometer, severely limiting the NR performance.
[27] K. Gloos, C. Mitschka, F. Pobell, and P. Smeibidl, Cryogenics **30**, 14 (1990).
[28] Heat conduction by free electrons becomes larger than phonons near 70 mK. Also, there will be some heat flow through the teflon spacers between NRs at high T_e.
[29] When the cryostat is tapped we observe larger warming spikes for F than the other chips [e.g., the dip in resistance near $B = 4$ T in Fig. 3(a) inset].